Willson, T., Hamerton, I., Varcoe, J., & Bance-Soualhi, R. (2019). Radiation-grafted cation-exchange membranes: an initial ex situ feasibility study into their potential use in reverse electrodialysis . *Sustainable Energy and Fuels*, *3*(7), 1682-1692.

Electronic supplementary information (ESI)

Radiation-grafted cation-exchange membranes: an initial *ex situ* feasibility study into their potential use in reverse electrodialysis

Terry R. Willson, Ian Hamerton, John R. Varcoe and Rachida Bance-Soualhi

This document provides additional data in support of the main article.

Synthesis of bis(vinylphenyl)ethane (BVPE) crosslinker

Bis(vinylphenyl)ethane (BVPE) was prepared *via* the Grignard coupling of 4-vinylbenzyl chloride (4-VBC) as reported by Li *et al.*[1] Mg turnings (1.0 g, 0.040 mol) were placed into a three-necked round-bottom flask along with 2–3 crystals of iodine, after which the flask was sealed and stirred for 1 h. Dry tetrahydrofuran (100 cm^3) was then added and the flask was purged and evacuated three times with N_2. 4-VBC (13 cm^3, 0.080 moles) was added dropwise to the flask (using a pressure equalised dropping funnel) while the temperature was maintained in the range -10 – 0 °C (using an NaCl(aq) ice bath). After addition of all of the 4-VBC, the reaction mixture was allowed to slowly raise to room temperature. After at least 16 h of stirring the reaction mixture was filtered to remove unreacted Mg followed by removal of the solvent under reduced pressure. The resulting residue was dissolved in dichloromethane and then washed several times with HCl (6 % vol.), water, and finally brine. The organic phase was dried over anhydrous MgSO4 before filtering and removal of solvent under reduced pressure. The resulting residue was recrystallised from hot methanol to recover the final BVPE product as a crystalline solid (5.6 g, 0.024 mol, 60 % yield).

NMR characterisation of the BVPE synthesised

The NMR spectral assignments given below (**A** – **F** and **a** – **g**) are highlighted in Fig. S1 (to the right).

^{1}H NMR ($CDCl_3$ with 1.0 % vol. TMS, 500.13 MHz ^{1}H resonance): δ_H = 7.38 (2H, d, J = 7.8 Hz, **A**), 7.18 (2H, d, J = 7.9 Hz, **B**), (1H, dd, J = 17.6, 10.9 Hz, **C**), 5.76 (1H, d, J = 17.6 Hz, **D**), 5.25 (1H, d, J = 10.9 Hz, **E**), and 2.95 (2H, s, **F**) ppm.

^{13}C NMR ($CDCl_3$, 125.76 MHz ^{13}C resonance): δ_C = 141.3 (**a**), 136.6 (CH, **b**), 135.3 (**c**), 128.6 (CH, **d**), 126.1 (CH, **e**), 113.0 (CH_2, **f**), and 37.5 (CH_2, **g**) ppm.

Raman (λ = 532 nm): 1630 (s), 1608 (s), 1565 (w), 1511 (w), 1426 (m), 1406 (m), 1326 (m), 1310 (m), 1200 (s), 1183 (s), 1007 (w), 910 (w), 867 (m), 824 (m), 774 (w), 724 (w), 641 (m) 566 (w), 444 (w), and 309 (m) cm^{-1}.

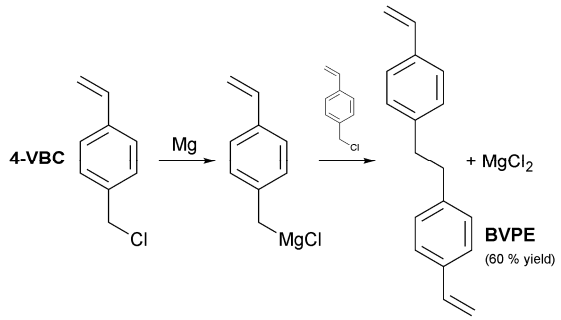

Scheme S1 An outline of the synthesis of BVPE crosslinker.

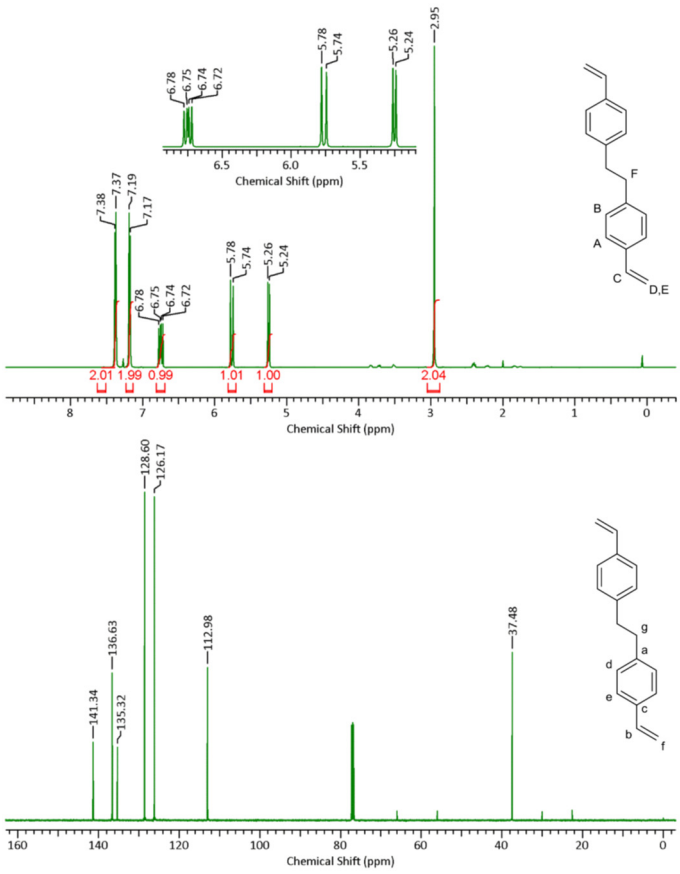

Fig. S1 ^{1}H and ^{13}C NMR spectra of the BVPE product obtained (Bruker 500 MHz spectrometer).

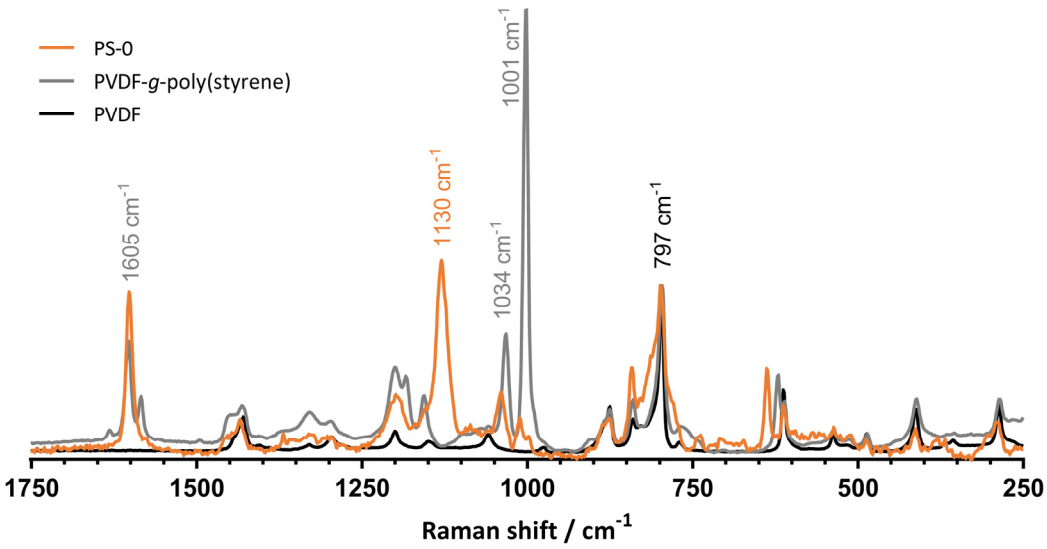

Fig. S2 The Raman spectra of the PVDF precursor film, PVDF grafted with styrene, and the final RG-CEM **PS-0**. Laser λ = 780 nm. Spectral intensities were normalised to the PVDF peak at 797 cm^{-1} to aid visual comparison. Full spectra characterisation can be found in ref. 2.

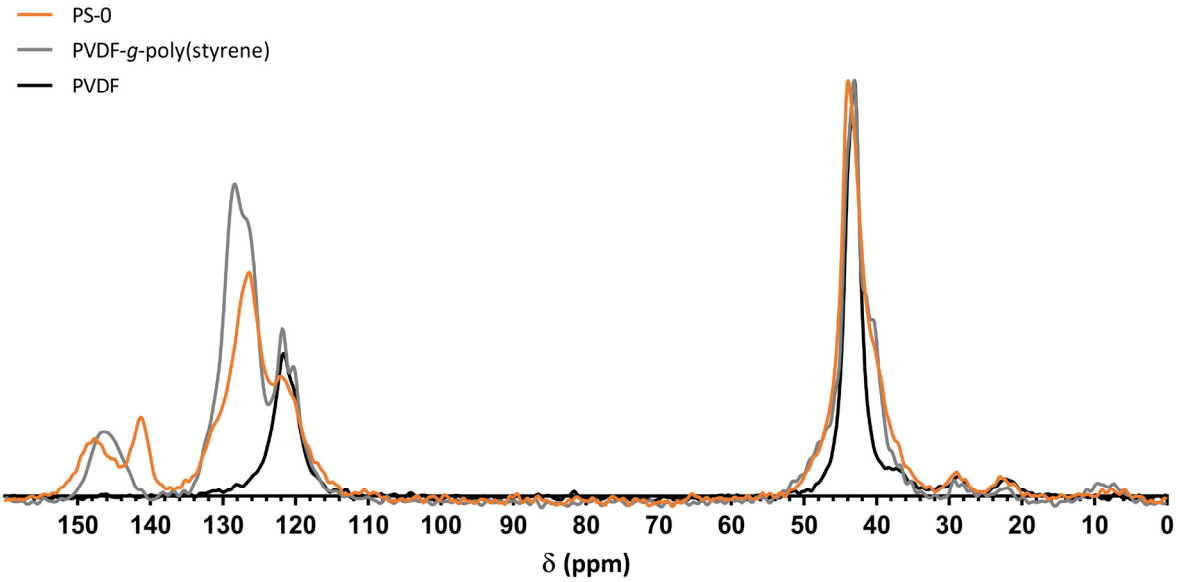

Fig. S3 The ^{13}C solid-state NMR of the PVDF precursor film, PVDF grafted with styrene, and the final RG-CEM **PS-0**. Spectral intensities were normalised to the PVDF peak at δ = 43 ppm to aid visual comparison. Full spectra characterisation can be found in ref. 2.

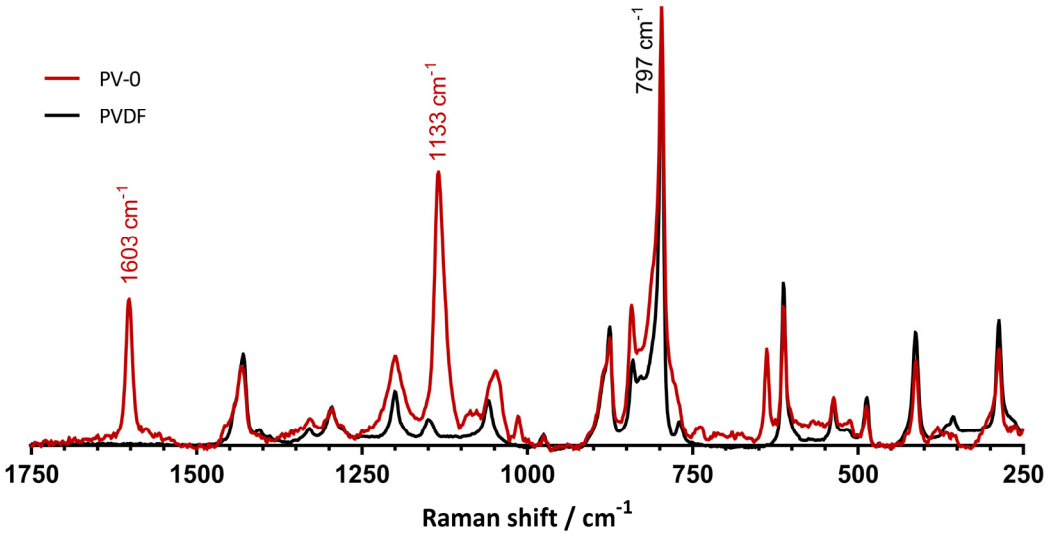

Fig. S4 The Raman spectra of the PVDF precursor film and the final RG-CEM **PV-0**. Laser λ = 780 nm. Spectral intensities were normalised to the PVDF peak at 797 cm^{-1} to aid visual comparison. Full spectra characterisation can be found in ref. 2.

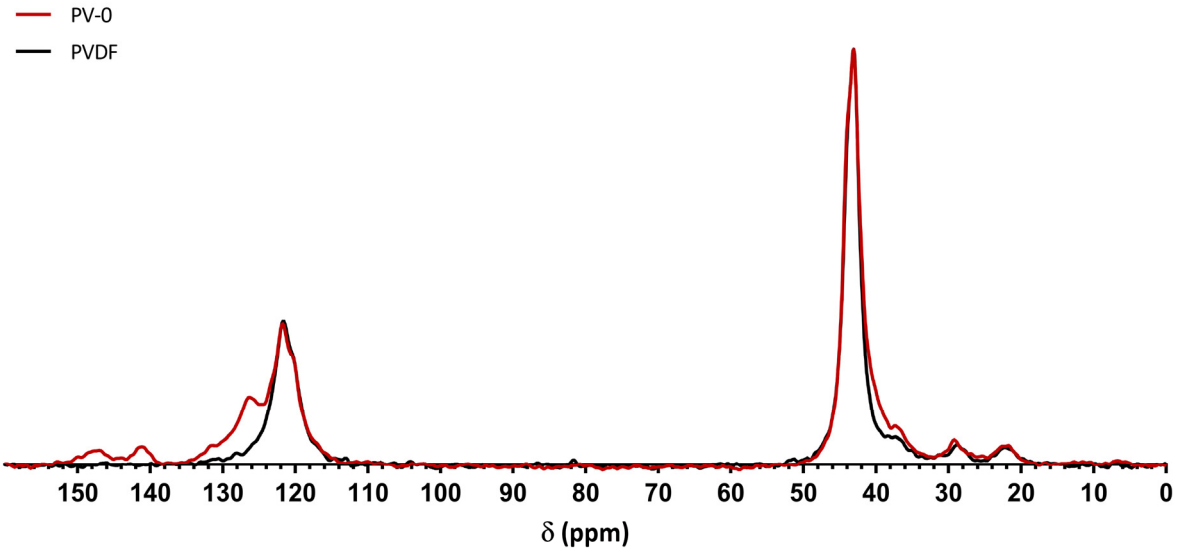

Fig. S5 The ^{13}C solid-state NMR of the PVDF precursor film and the final RG-CEM **PV-0**. Spectral intensities were normalised to the PVDF peak at δ = 43 ppm to aid visual comparison. Full spectra characterisation can be found in ref. 2.

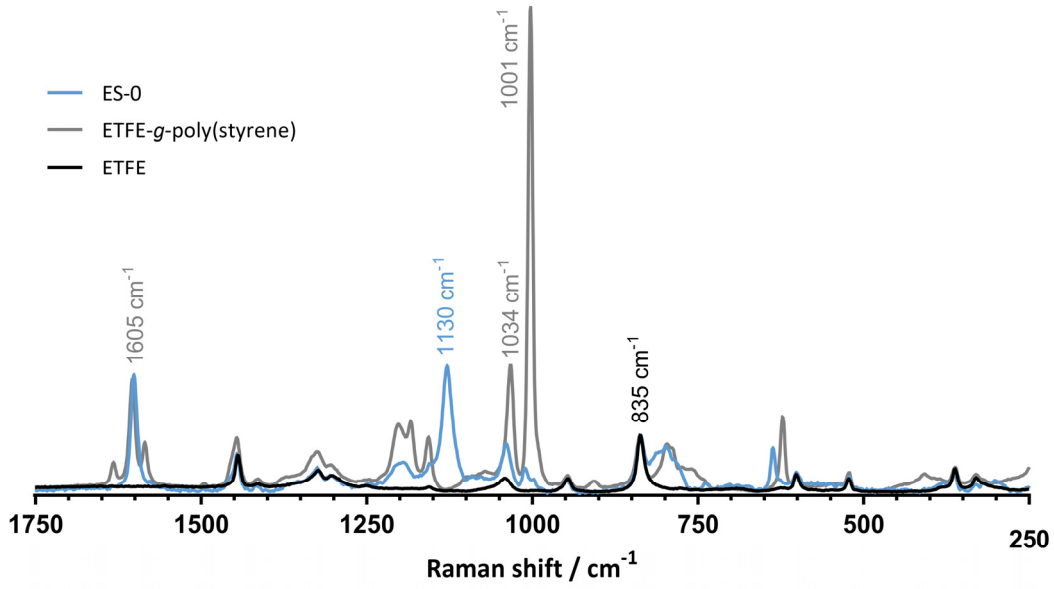

Fig. S6 The Raman spectra of the ETFE precursor film, ETFE grafted with styrene, and the final RG-CEM **ES-0**. Laser λ = 780 nm. Spectral intensities were normalised to the ETFE peak at 835 cm^{-1} to aid visual comparison. Full spectra characterisation can be found in ref. 2.

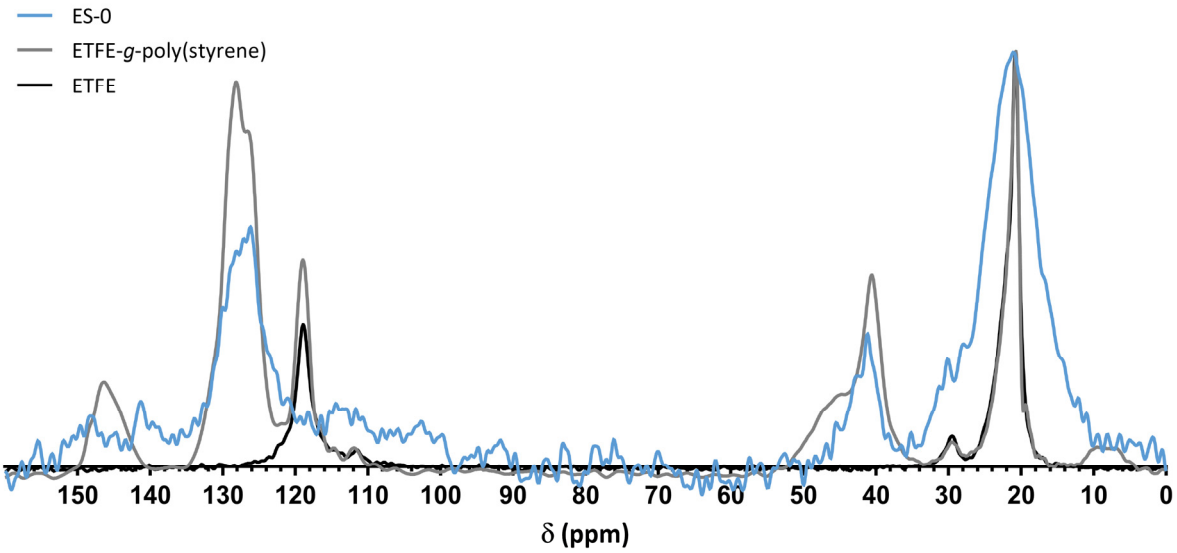

Fig. S7 The ^{13}C solid-state NMR of the ETFE precursor film, ETFE grafted with styrene, and the final RG-CEM **ES-0**. Spectral intensities were normalised to the ETFE peak at δ = 21 ppm to aid visual comparison. Full spectra characterisation can be found in ref. 2.

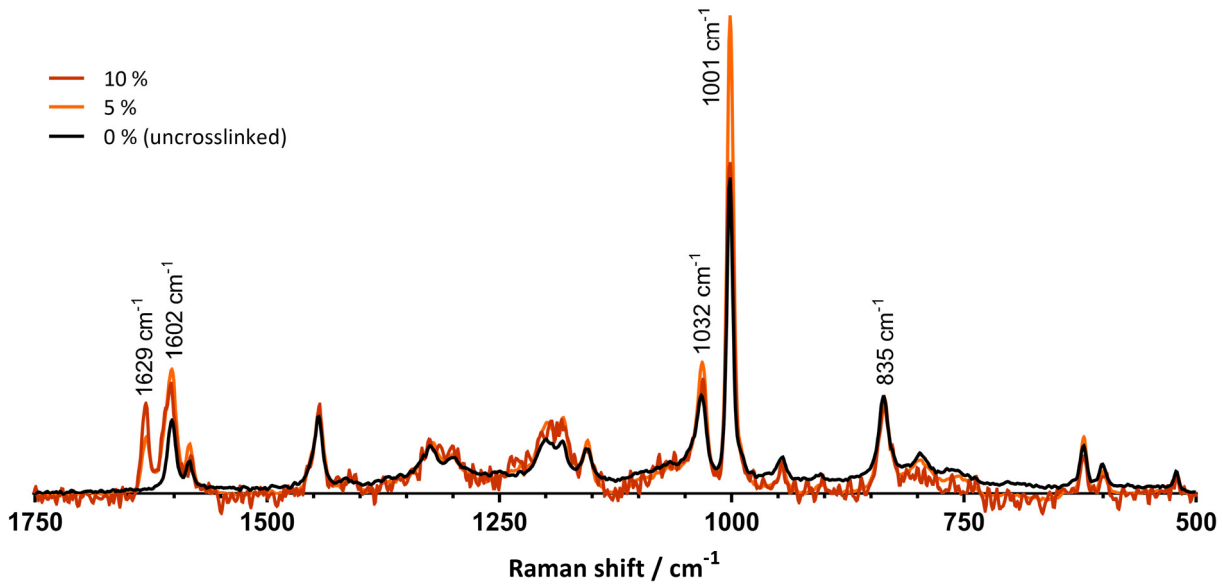

Fig. S8 The Raman spectra of the pre-sulfonated ETFE-*g*-poly(styrene-co-DVB) films used to form **ES-D0**, **ES-D5**, and **ES-D10**. Laser λ = 532 nm. Spectral intensities were normalised to the ETFE peak at 835 cm^{-1} to aid visual comparison. Full spectra characterisation can be found in ref. 2.

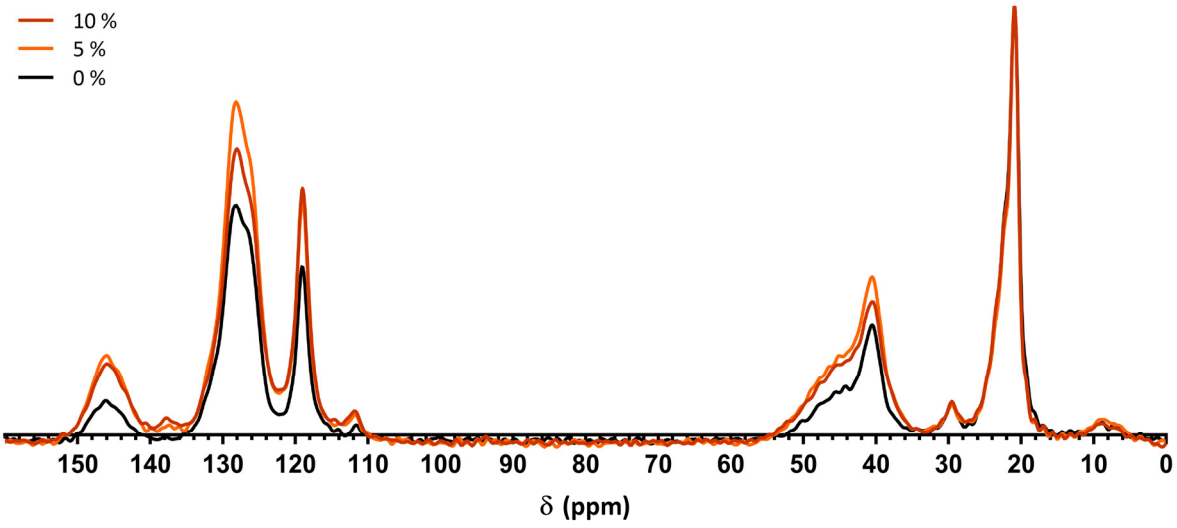

Fig. S9 The ^{13}C solid-state NMR of the pre-sulfonated ETFE-*g*-poly(styrene-co-DVB) films used to form **ES-D0**, **ES-D5**, and **ES-D10**. Spectral intensities were normalised to the ETFE peak at δ = 21 ppm to aid visual comparison. Full spectra characterisation can be found in ref. 2.

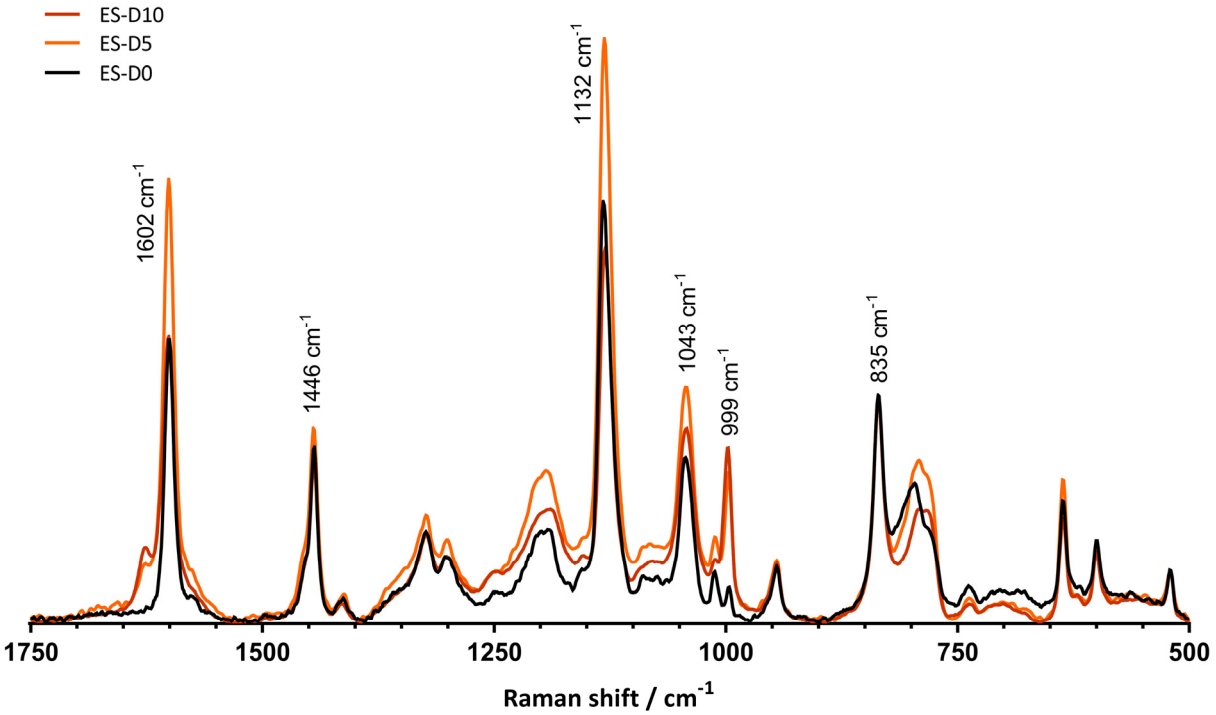

Fig. S10 The Raman spectra of **ES-D0**, **ES-D5**, and **ES-D10**. Laser λ = 785 nm. Spectral intensities were normalised to the ETFE peak at 835 cm^{-1} to aid visual comparison.

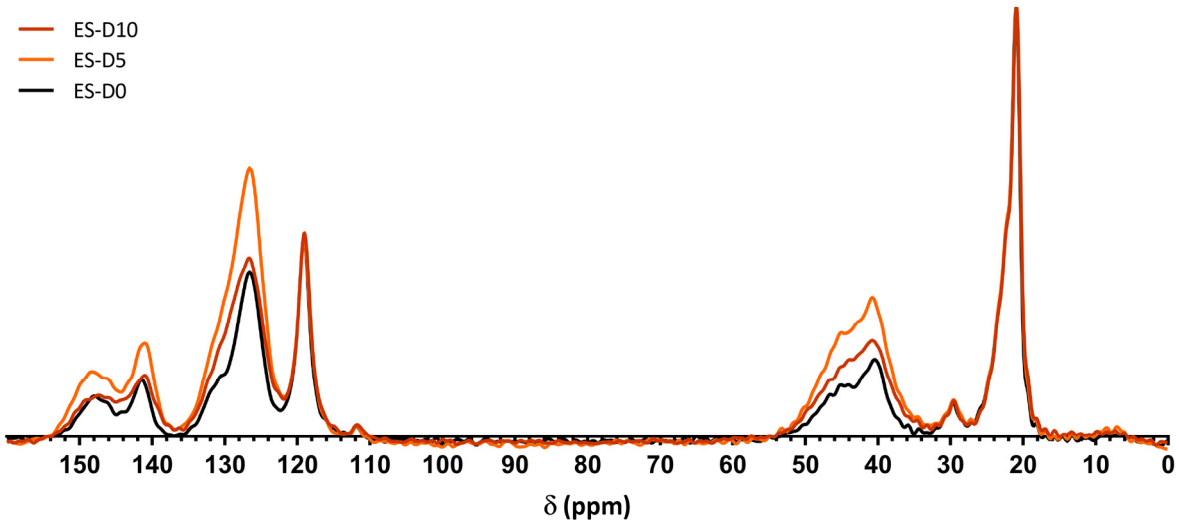

Fig. S11 The ^{13}C solid-state NMR of **ES-D0**, **ES-D5**, and **ES-D10**. Spectral intensities were normalised to the ETFE peak at δ = 21 ppm to aid visual comparison. Full spectra characterisation can be found in ref. 2.

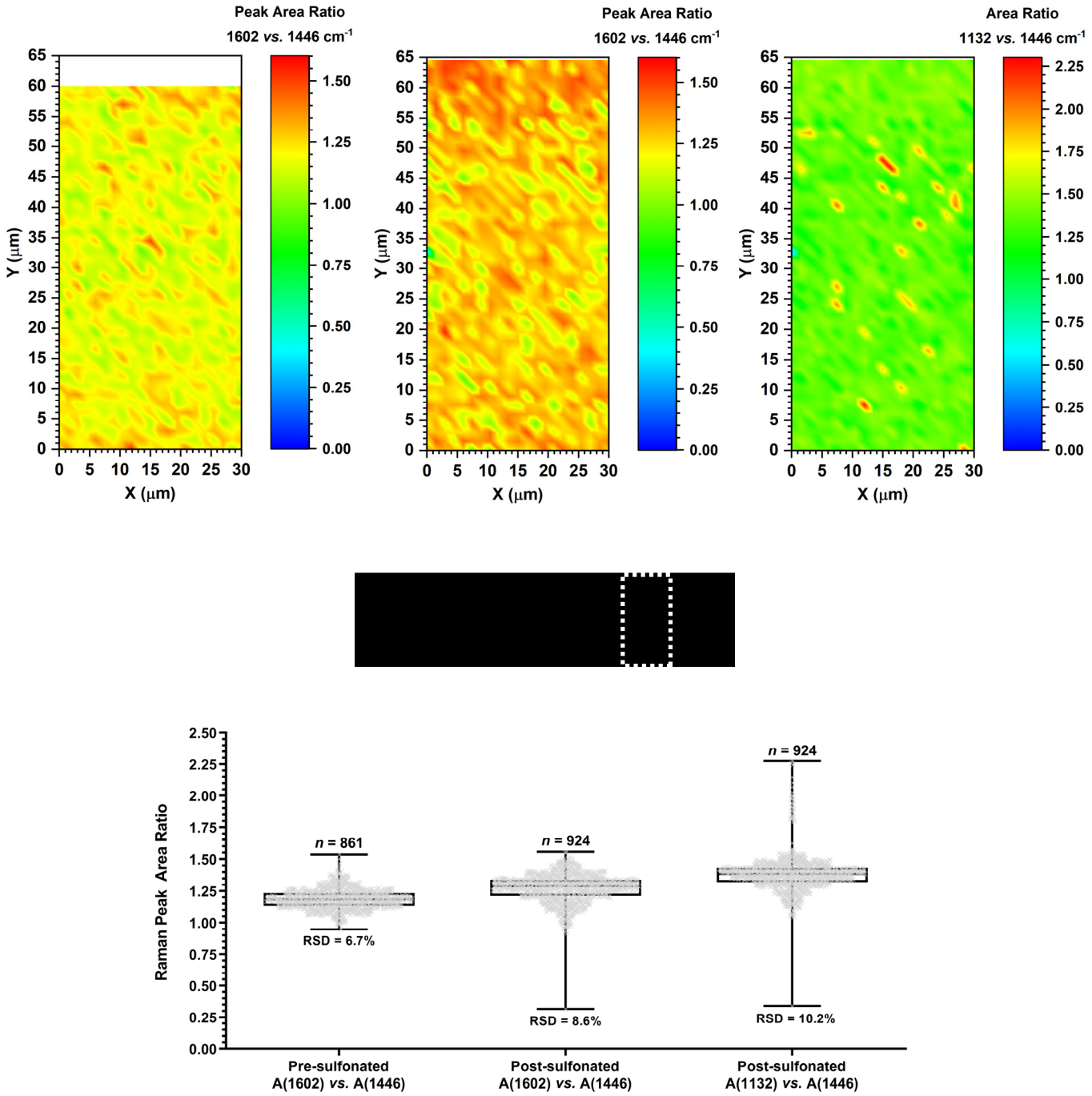

Fig. S12 The top row presents the Raman microscopy cross-sectional maps of samples of: (left map) pre-sulfonated ETFE-*g*-poly(styrene-co-BVPE) films used to form **ES-B10**; and (middle and right maps) **ES-B10** (air dried). The instrument used was a Renishaw InVia Reflex Raman Microscope with an NA = 0.75 (50 ×) objective and a λ = 785 nm laser (calculated laser spot (Airy disk) diameter of 1.28 μm):[3] the sample stage (x-y) step size was 1.5 μm. The y-axis is the through core direction (see the cartoon in the middle where the white dashed box indicates the sample areas that were mapped). Note the pre-sulfonated sample was *ca.* 5 μm thinner (y-axis direction) than the dry sulfonated sample. The colour scales represent the integrated area ratios between the indicated peaks: 1442 cm^{-1} (stemming from the precursor ETFE film component), 1602 cm^{-1} (aromatic ring peaks due to the grafted chains), and 1132 cm^{-1} (sulfonate groups). The bottom graph presents the peak area ratio data for the three Raman maps in box and whisker plot format giving the minimum, interquartile range (box), medians (horizontal line in the boxes), and maximum values (along with the individual data points in grey). The relative standard deviations (RSD) are used as a proxy measurement of the inhomogeneity of functionalisation. The dry (post-sulfonated) **ES-B10** cross-section sampled contained a small defect (at X = 0 and Y = 33 μm in the Raman maps), which accounts for the minimum outlier values in the respective box and whisker plots.

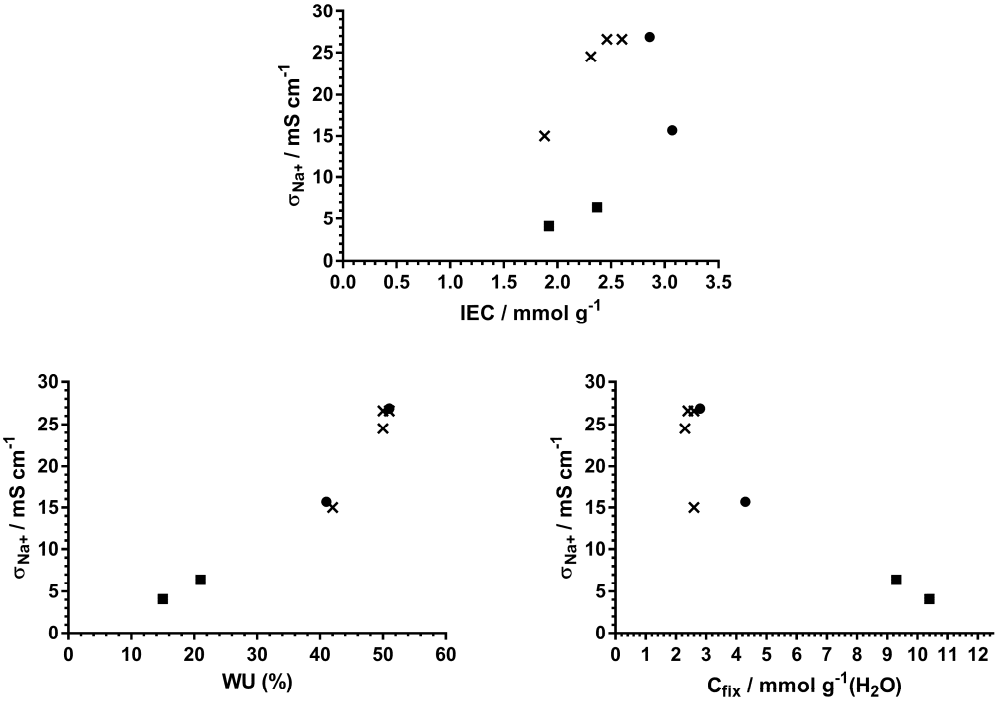

Fig. S13 The effects of IEC, WU, and C_{fix} on the room temperature, through-plane (in water) Na^+ conductivities of all of the RG-CEMs reported in Tables 1 – 3 in the main article: ✖ = uncrosslinked variants, ■ = DVB-crosslinked variants, and ● = BVPE-crosslinked variants.

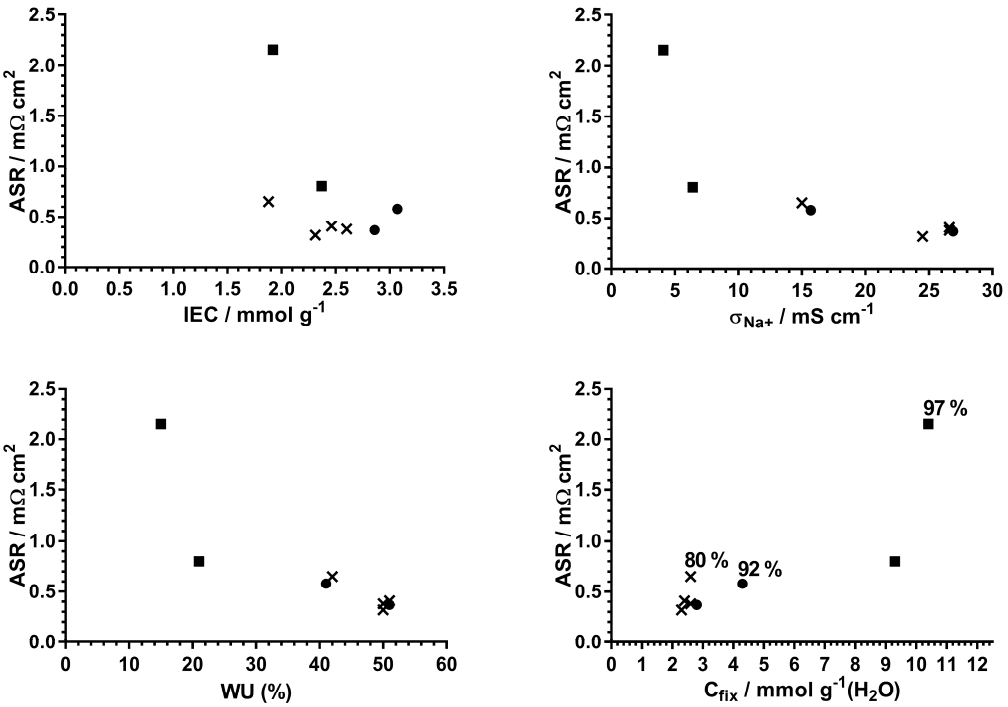

Fig. S14 The effects of IEC, WU, σ_{Na+} and C_{fix} on the area specific resistances (ASR) of the Na^+ form RG-CEMs in water: ✖ = uncrosslinked variants, ■ = DVB-crosslinked variants, and ● = BVPE-crosslinked variants. Select permselectivies (α) are given in the C_{fix} plot.

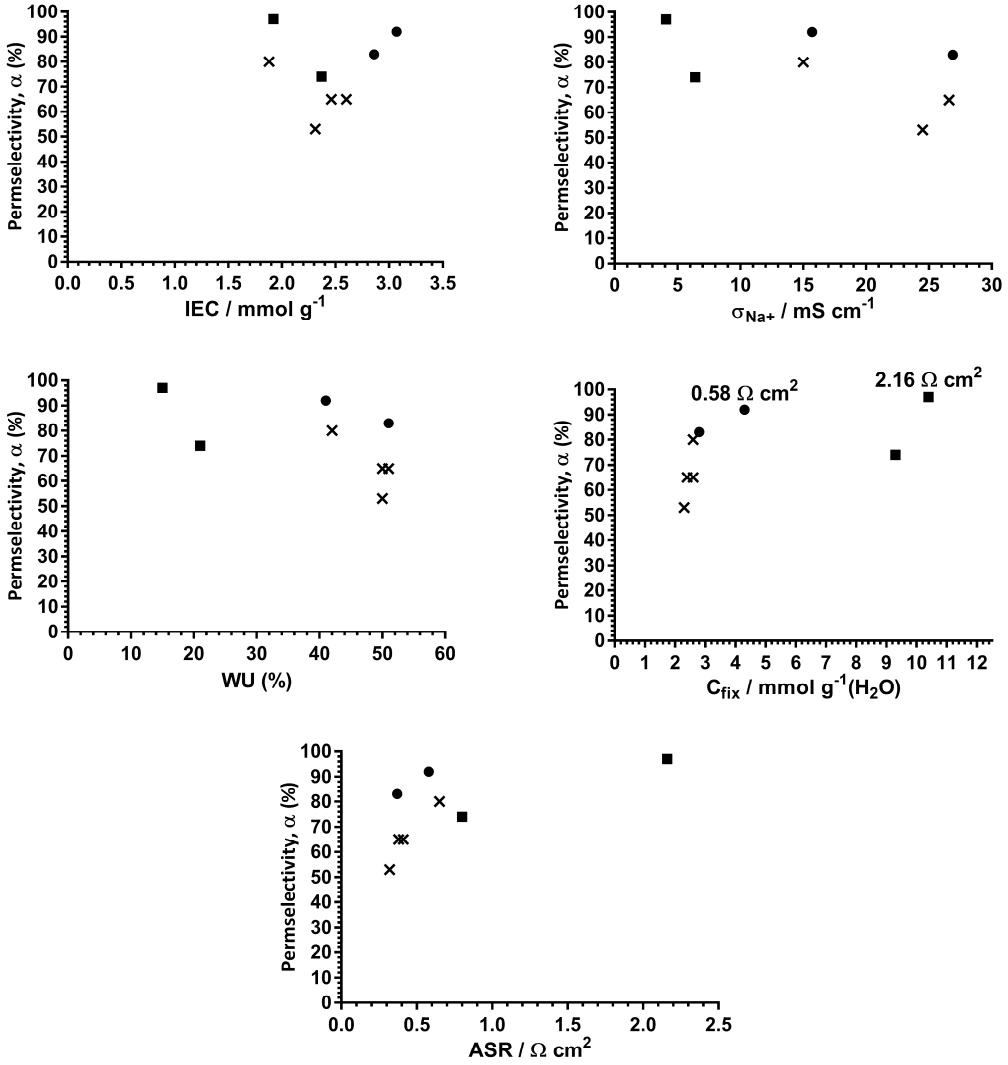

Fig. S15 The effects of IEC, WU, σ_{Na+}, C_{fix} and ASR on the permselectivies (α) of the RG-CEMs reported in Tables 1 – 3 in the main article: ✖ = uncrosslinked variants, ■ = DVB-crosslinked variants, and ● = BVPE-crosslinked variants. Select ASR values are given in the C_{fix} plot.

References to the ESI

1 W.-H. Li, K. Li, H. D. H. Stover and A. E. Hamielec, *J. Polym. Sci.: Part A*: *Polym. Chem.*, 1994, **32**, 2023.
2 T. R. Willson, PhD Thesis, The University of Surrey, 2018 (available at http://epubs.surrey.ac.uk/id/eprint/846392).
3 W. H. Lee, C. Crean, J. R. Varcoe, R. Bance-Soualhi, *RSC Adv.*, 2017, **7**, 47726.